Hindawi
International Journal of Photoenergy
Volume 2022, Article ID 3441926, 13 pages
https://doi.org/10.1155/2022/3441926

Research Article

Analysis of the Refrigeration Performance of the Refrigerated Warehouse with Ice Thermal Energy Storage Driven Directly by Variable Photovoltaic Capacity

Junyu Liang,[1] **Wenping Du**,[2,3] **Dada Wang**,[1] **Xingyu Yuan**,[1] **Mei Liu**,[4] **and Kunhao Niu**[4]

[1]*Electric Power Research Institute of Yunnan Power Grid Co., Ltd, Kunming 650217, China*
[2]*Chuxiong Normal University, Chuxiong 675000, China*
[3]*School of Energy and Environmental Science, Yunnan Normal University, Kunming 650500, China*
[4]*Qujing Bureau, EHV Power Transmission Company of CSG, Qujing 655000, China*

Correspondence should be addressed to Wenping Du; 597957176@qq.com

Received 1 April 2022; Revised 27 October 2022; Accepted 17 November 2022; Published 30 November 2022

Academic Editor: Ahmad Umar

An independent solar photovoltaic (PV) refrigerated warehouse system with ice thermal energy storage is constructed in this paper. In this system, the vapour compression refrigeration cycle is directly driven by a PV array, and the frequency of the compressor varies with the solar radiation intensity. The refrigeration performance and the matching characteristics of the system driven by different PV capacities are studied. The results show that the intensity of solar radiation required for the compressor to work at the same frequency decreases by approximately 7.8% when the ratio of PV capacity to compressor-rated power increases by 10%, and the time required for the temperature in the refrigerated warehouse to drop from ambient temperature to 0°C is reduced by 32 min on average. The energy efficiency ratio of the vapour compression refrigeration subsystem and the coefficient of performance (COP) of the refrigerated warehouse system increase with the ratio of PV capacity to compressor-rated power α. When α increases from 1 to 1.3, the growth rate of the COP is very slow. For the PV direct-drive refrigerated warehouse system with a compressor-rated power of 4.4 kW, the suitable ratio of PV capacity to compressor-rated power α is about 1.3. When the refrigerated warehouse system is driven directly by a 5.4 kW PV array, the overall COP is approximately 0.19. In the cycle mode of refrigeration and cold energy storage during the day and cold energy release at night, the stored cold energy can still meet the refrigeration required by the load for 48 hours after eight days of continuous operation. According to the current market price of cold storage, during the service life of the system, the income per unit volume of cold storage is about 2.2 times the investment.

1. Introduction

With the improvement in living standards, the demand for fresh fruits and vegetables is also higher. However, agricultural products are still alive after they are harvested; it is a great challenge to maintain the nutrition and fresh quality of agricultural products after being harvested due to their perishable nature [1]. Huge losses in fruits and vegetables have been caused by improper processing and a lack of adequate refrigeration infrastructure and cold chain logistics facilities [2]. Fruit and vegetable loss accounts for 40-50% of annual food loss by weight worldwide [3, 4]. Currently, the postharvest wastage rate of agricultural products is still high [5], and the distribution of a large number of agricultural products in rural areas is hampered by inadequate refrigeration infrastructure and poor electricity supply. Temperature management is considered to be the most important factor in controlling the deterioration of the physiology and pathology of agricultural products [6]. Low temperature reduces respiratory intensity and metabolism

and inhibits bacterial reproduction, thus slowing spoilage [7]. At the same time, concern for energy shortages and environmental degradation has made green refrigeration a consensus. The good matching of solar energy resources and refrigeration requirements makes solar refrigeration one of the preferred refrigeration solutions.

Solar refrigeration can be divided into solar thermal refrigeration and solar-electric refrigeration [8]. Solar PV (photovoltaic) refrigeration uses electric energy to drive the vapour compression refrigeration cycle with high energy efficiency ratio, and with the reduction of PV module cost and improvement of efficiency, solar PV refrigeration is considered to have greater application potential [9]. Solar PV refrigeration combined with vapour compression refrigeration cycle can be divided into grid-connected photovoltaic refrigeration system and independent photovoltaic refrigeration system according to the power supply mode [10]. Independent photovoltaic cooling technology can build the system according to the actual cooling demand, and the system is more flexible, especially in remote areas without power grids. Therefore, independent photovoltaic cooling technology is considered to have more application potential [8].

As early as 2009, Modi et al. [11] redesigned a 165 L traditional household refrigerator into a solar-powered refrigerator by adding battery packs, inverters, and transformers. The solar refrigerator reached the maximum COP of 2.10 at 7:00 am. Currently, researchers have researched photovoltaic air conditioning [12, 13], solar ice makers [14, 15], and solar refrigerators [11, 16]. The system performance of the solar photovoltaic refrigeration system with the battery bank was studied by researchers. Lei et al. [17] studied a photovoltaic driven miniature refrigeration system. Under cloudy and sunny weather conditions, the average cooling output of the system was 416 W and 399 W, and the corresponding average COP was 3.42 and 3.02, respectively. Torres-Toledo et al. [18] conducted an experimental study on the milk cooling performance of a PV-DC refrigeration system applied to a small farm milk tank. Using an insulated milk tank with an integrated ice tray to transport milk in the morning and store it in the evening, 8 kg of ice was produced, keeping 30 L of milk at low temperature and effectively preventing bacterial reproduction [19].

In these independent photovoltaic refrigeration systems, the battery bank serves as an essential energy storage unit to ensure stable and continuous operation due to the inherent intermittency and unstable nature of solar energy [10]. However, there is a problem that cannot be ignored; the battery life is much shorter than that of PV modules in such systems. Frequent replacement of batteries increases the investment and operating cost of the system and may cause environmental pollution [14, 20].

The researchers studied the battery-free solar independent photovoltaic refrigeration system to eliminate the use of batteries and charging controllers and their associated economic and environmental problems. El-Bahloul et al. [21] conducted experimental studies on solar DC vapour compression refrigerators with/without phase change energy storage materials in dry hot areas, and the results showed that COP was higher without phase change energy storage materials, but when there was a lack of solar radiation, the temperature in the refrigerator changed rapidly due to the absence of phase change energy storage materials and other compensations; when the refrigerator with phase change energy storage materials operates at full load outdoors, the COP is 1.22. Mishra et al. [22] constructed an independent photovoltaic cold storage system using a split household air conditioner, and the refrigerator was integrated with sensors based on the Internet of Things for remote monitoring of temperature, humidity, and stored items; the average annual utilization rate of 10-ton cold storage in India is 70% and the payback period is 2.1 years. Axaopoulos and Theodoridis [14] designed a battery-free solar photovoltaic driven ice-making system, using a dedicated controller to provide power management for the four compressors, and the efficiency from solar to the compressor is about 9.2%.

Meanwhile, some studies have compared the performance of the battery, ice, and phase change materials as an energy storage unit in the independent photovoltaic refrigeration system. The results show that the power consumption of the ice thermal storage system and the phase change material storage system is 4.59% and 7.58% lower than that of the conventional storage battery, respectively, and the ice thermal storage system and the phase change material storage system can significantly reduce CO_2 emissions [23]. Primary energy saving rates for the battery as the energy storage and phase change material as cold energy storage are 2.8 times and 1.9 times higher than those without energy storage, respectively [24]. Luerssen et al. [25] proposed a tiered storage cost model to compare electrical and thermal energy storage for refrigeration applications. The results indicate that thermal energy storage has greater potential for applications with larger cooling demands, such as hotels and refrigerated warehouses. In addition, ice storage technology can help reduce the maximum capacity of cooling equipment [26].

Based on the analysis above, it is not difficult for us to conclude that solar PV refrigerated warehouse meets the requirements of green refrigeration and has great development potential. Actively developing solar photovoltaic refrigerated warehouses has great social and economic benefits in reducing the loss of fruits and vegetables after harvest [17]. Our research group carried out research work on the PV direct-drive air-conditioning system with ice-making and verified the feasibility of ice thermal energy storage instead of battery energy storage in a stand-alone PV system [27, 28]. And, under the impedance matching strategy, the system can provide continuous cooling for a room of 25.5 m^2 for 8.5 hours [13].

Based on the previous work of the research group, in this paper, a photovoltaic direct-drive vapour compression refrigeration refrigerated warehouse system combined with ice thermal energy storage technology is proposed, which can store excess cold energy while supplying cooling. To obtain the refrigeration performance influence rule and matching characteristics of the constructed refrigerated warehouse system driven by different PV capacities under different irradiation conditions, theoretical analysis and experimental study on sunny and cloudy were carried out

in this paper. The purpose of this paper is to provide some references for the application of the independent photovoltaic direct-drive refrigerated warehouse system.

2. System Description

2.1. Components of the Refrigerated Warehouse System and Working Principle. The independent PV refrigerated warehouse system with ice thermal energy storage consists of three parts: PV power generation subsystem, vapour compression refrigeration subsystem, and ice thermal energy storage and cooling subsystem. Among them, the PV power generation subsystem includes PV arrays and inverter controllers; the vapour compression refrigeration subsystem includes variable frequency compressors, condensers, expansion valves, and air coolers; ice thermal energy storage and cooling subsystem include ice storage tanks, working medium pump, and fan coil. The schematic diagram of the independent PV refrigerated warehouse system with ice thermal energy storage is shown in Figure 1.

The operation process of the system is as follows: in the daytime, the PV array converts solar energy into direct current, and the inverter controller converts the direct current into a three-phase alternating current to drive the vapour compression refrigeration cycle. To enable the compressor to operate stably under irradiance fluctuations, the system adopts maximum power point tracking technology to ensure optimal energy conversion and a stable power supply. In the vapour compression refrigeration cycle, the refrigerant is compressed into high-temperature and high-pressure gas in the compressor and then condensed into medium-temperature and high-pressure liquid in the air condenser. After being throttled by the throttling valve, the refrigerant is a low-temperature and low-pressure liquid. The refrigerant flows into the interior of the air cooler in the refrigerated warehouse to absorb the heat of air to cool the refrigerated warehouse; then the refrigerant flows through the ice-making evaporator in series with the air cooler. When the refrigerant flows through the ice-making evaporator immersed in water, it continuously absorbs the heat of the water in the ice storage tank, then the water phase transition in the ice storage tank and the excess cold energy is stored in the form of ice thermal energy. Under the condition of lack of solar irradiance during the day or no solar irradiation at night, the refrigerated warehouse can adjust the circulating pump according to temperature to melt ice and release cold energy. The cold exchange coil pumps the cold energy stored in the ice storage tank to the fan coil to supply cold to the cold storage, thus achieving continuous and stable cooling.

2.2. System Performance. To determine the matching relationship between the PV capacity and the compressor-rated power, the ratio between the PV capacity P_{PV} and the compressor-rated power P_{comp} is defined as the system capacity ratio, which is expressed by α, namely:

$$\alpha = \frac{P_{\mathrm{PV}}}{P_{\mathrm{comp}}}. \tag{1}$$

PV arrays with capacities of 4.5 kW, 5.4 kW, and 6.6 kW are used as driving energy sources, respectively, and the photoelectric and refrigeration performance of the system is studied.

2.2.1. Photoelectric Performance. The power quality of PV power generation can be evaluated according to the three-phase current and voltage imbalance proposed by the International Council on Large Electric Systems. The specific expression is as follows [29]:

$$\varepsilon_I = 3 \times \frac{\mathrm{Max}(I_1, I_2, I_3) - \mathrm{Min}(I_1, I_2, I_3)}{I_1 + I_2 + I_3}, \tag{2}$$

$$\varepsilon_U = 3 \times \frac{\mathrm{Max}(U_1, U_2, U_3) - \mathrm{Min}(U_1, U_2, U_3)}{U_1 + U_2 + U_3}, \tag{3}$$

where I_1, I_2, and I_3 are the three-phase current output of the inverter controller, A; U_1, U_2, and U_3 are the effective three-phase voltage output of the inverter controller, V.

The calculation formula for photoelectric conversion efficiency is [9]:

$$\eta_{\mathrm{pv}} = \frac{Q_{\mathrm{pv}}}{q_{\mathrm{pv}} \times S_{\mathrm{pv}}}.100\%. \tag{4}$$

Compressor utilization efficiency is expressed as

$$\eta = \frac{Q_{\mathrm{comp}}}{q_{\mathrm{pv}} \times S_{\mathrm{pv}}}. \tag{5}$$

In the formula, Q_{PV} is PV array energy output, MJ; q_{PV} is cumulative solar radiation received per unit area of the PV module, MJ/m^2; S_{PV} is PV array area, m^2; Q_{comp} is compressor energy consumption, MJ.

2.2.2. Refrigeration Performance. The cold energy stored in the photovoltaic refrigerated warehouse system in no-load mode includes the cold energy of water in the ice storage tank, the change in latent heat of the water phase to ice, a small amount of the cold energy of supercooled ice, the cooling consumption of air in the refrigerated warehouse, and the cooling loss through the maintenance structure. The calculation formula can be expressed as follows:

$$\begin{aligned} Q_{\mathrm{ref}} = {} & \int_{T_{\mathrm{bw}}}^{T_{\mathrm{ew}}} (C_w m_w)\mathrm{d}T + \int_{T_{\mathrm{bw}}}^{0} (C_w m_{\mathrm{ice}})\mathrm{d}T + m_{\mathrm{ice}} h_{\mathrm{wi}} \\ & + \int_{0}^{T_{\mathrm{ew}}} (C_i m_{\mathrm{ice}})\mathrm{d}T + \int_{T_{\mathrm{bc}}}^{T_{\mathrm{ec}}} (C_v m_{\mathrm{air}})\mathrm{d}T \\ & + \int_{T_{\mathrm{bc}}}^{T_{\mathrm{ec}}} \mathrm{KA}a(T_o - T_i)\mathrm{d}T. \end{aligned} \tag{6}$$

In the formula, Q_{ref} is the cold energy, MJ; C_w is the specific heat capacity of water, 4.2×10^3 J/(kg·°C); m_w is the mass of water in the ice storage tank at the end of the experiment, kg; T_{bw} is the temperature of the water

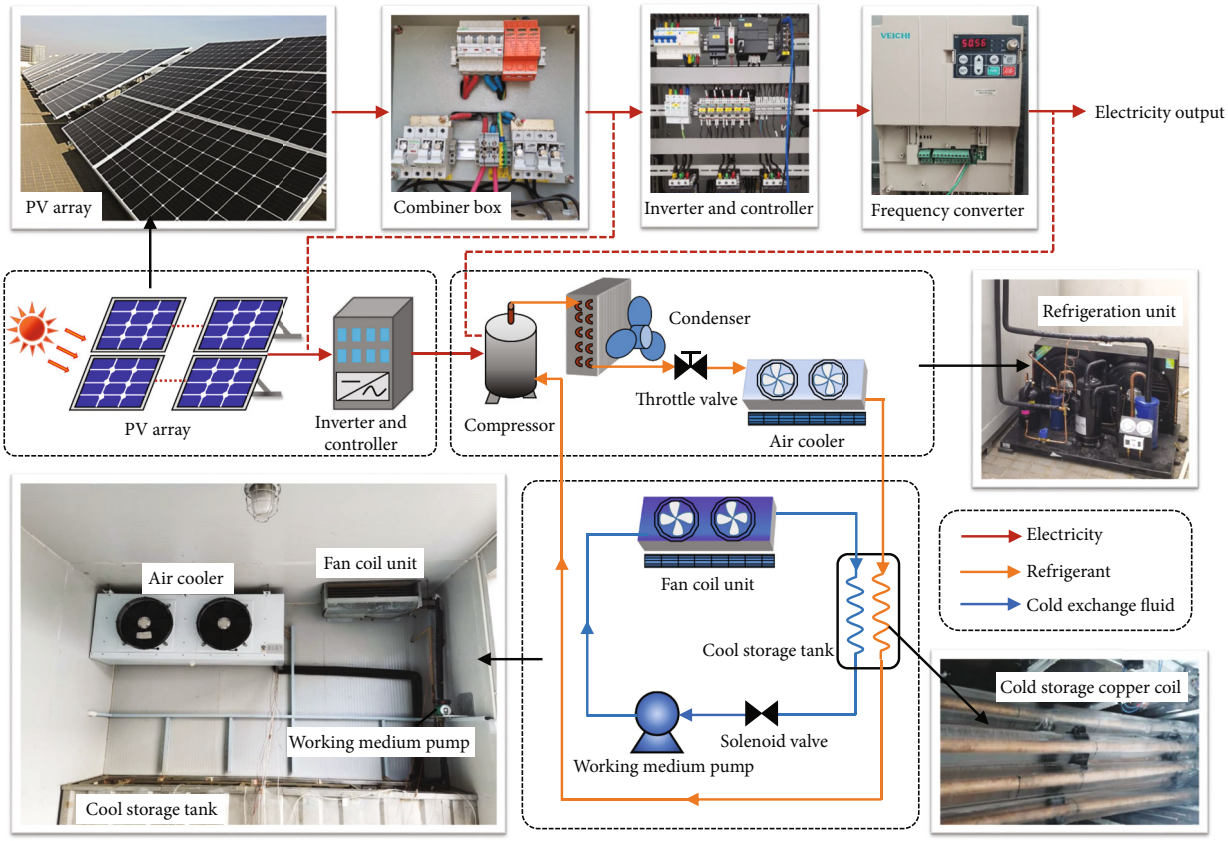

Figure 1: Schematic diagram of the photovoltaic refrigerated warehouse system with ice thermal energy storage.

at the beginning of the experiment, ˚C; T_{ew} is the temperature of the water at the end of the experiment, ˚C; m_{ice} is the mass of ice, kg; T_{ei} is the temperature of the ice at the end of the experiment, ˚C; C_i is the specific heat capacity of ice, 2.1×10^3 J/(kg·˚C); h_{wi} is the latent heat of the phase transition between ice and water, 3.36×10^3 J/kg; T_{bc} is the temperature of the refrigerated warehouse at the beginning of the experiment, ˚C; T_{ec} is the temperature of the refrigerated warehouse at the end of the experiment, ˚C; C_v is the specific heat capacity of air, 1.005×10^3 J/(kg·˚C); m_{air} is the air mass in the refrigerated warehouse, kg; K is the heat transfer coefficient of the refrigerated warehouse maintenance structure, W/(m^2·˚C); A is the area of the refrigerated warehouse maintenance structure, m^2; a is the temperature difference correction coefficient on both sides of the maintenance structure; T_o is the temperature outside the maintenance structure, ˚C; T_i is the temperature inside the maintenance structure, ˚C; t_a and t_b are the time when the experiment begins and ends.

The coefficient of performance (COP) of the independent PV refrigerated warehouse system is the ratio of the refrigerating capacity of the system to the solar radiation received by the PV array. The refrigeration performance of the vapour compression refrigeration subsystem is expressed by the energy efficiency ratio (EER), that is, the ratio between the refrigerating capacity and the energy consumption of the compressor, which can be calculated using the following formula [27]:

$$\mathrm{COP} = \frac{Q_{\mathrm{ref}}}{q_{\mathrm{pv}} \times S_{\mathrm{pv}}}, \tag{7}$$

$$\mathrm{EER} = \frac{Q_{\mathrm{ref}}}{Q_{\mathrm{comp}}}. \tag{8}$$

In the formula, Q_{comp} is the compressor energy consumption, MJ.

Cooling capacity supply performance is one of the important indicators of refrigerated warehouse system performance. The average cooling capacity supply of units of space per minute is expressed by Q_{ave}, and its calculation formula is the following:

$$Q_{\mathrm{ave}} = \frac{Q_{\mathrm{ref}}}{V_{\mathrm{hou}} \times H_{\mathrm{pv}}}. \tag{9}$$

In the formula, V_{hou} is the volume of the refrigerated warehouse, m^3; H_{pv} is the system uptime, min.

2.3. Experiment and Testing Instrument. The volume of the constructed PV refrigerated warehouse is 24.47 m^3, and the capacity of the PV array is adjustable from 4.5 to 6.6 kW.

Table 1: Experimental device and its parameters.

Subsystem	Main components	Model	Parameter value
PV power generation subsystem	PV module	STP300S-20	V_{mp}: 32.6 V; I_{mp}: 9.21 A P_{max}: 300 W
	Inverter and controller	HPS30	U_{in}: 480-820 V; U_{out}: 380 V ± 5%
Refrigeration subsystem	Compressor	503DHV-80D2	f: 10-50 Hz; U: 380 V; P: 4.4 kW
	Condenser	FNF-10.2/50	P: 0.4 kW
	Air cooler	DJ-30	Q: 4.3 kW; q: 7000 m/h
	Working fluid pump	SRS25/7-130	P_{in}:118 W; q: 62 L/min
Cold energy storage and supply subsystem	Fan coil	FP-68	q: 680 m^3/h
	Ice storage tank	/	V: 0.72 m^3

Table 2: Parameters of the experimental test instrument.

Device	Model	Measuring range	Accuracy
Meteorological monitoring station	TYD-ZS2	0-2000 W/m^2	±5%
Temperature test instrument	CSG solar test system	-50-200°C	±0.1 °C
Electronic balance	Naikesi	0-100 kg	0.001 kg

The experimental device and its parameters are shown in Table 1.

The maximum power point tracking technology is adopted in the system to ensure that the PV array optimizes solar energy into electric energy under the condition of fluctuation of irradiance. The compressor variable frequency operates according to the photovoltaic output power. During the experiment, the data collector recorded the temperature of the refrigerant at the inlet and outlet of the compressor, the temperature of the refrigerant at the inlet and outlet of the condenser, the temperature of the refrigerant at the inlet and the outlet of the evaporator, the water temperature in the upper, middle, and lower positions of the ice storage tank, and the ice temperature and the internal temperature of the refrigerated warehouse. The PV output voltage, current, and power of the compressor as well as the frequency of the compressor during the operation of the system are automatically recorded and stored by the computer software through the sensor. The main instrument models, parameters, and accuracy of the experimental test instrument are shown in Table 2.

2.4. Uncertainty Analysis. Uncertainty is an important parameter to analyse the experimental results. The accuracy of the instrument, the operating environment, the location of the test points, and the observation method can cause experimental errors. formula (7) shows that the measurement error of the system COP is affected by the uncertainty of the cooling capacity of the system Q_{ref}, cumulative solar radiation q_{pv}, and the area of photovoltaic module S_{pv}. The uncertainty of the system COP is calculated by equation (10) [30, 31]:

$$w_{COP} = \sqrt{\left(\frac{\partial COP}{\partial Q_{ref}} w_{Q_{ref}}\right)^2 + \left(\frac{\partial COP}{\partial q_{pv}} w_{q_{pv}}\right)^2 + \left(\frac{\partial COP}{\partial S_{pv}} w_{S_{pv}}\right)^2}. \tag{10}$$

In formula (10), $w_{Q_{ref}}$, $w_{q_{pv}}$, and $w_{S_{pv}}$ represent the error of the system cooling capacity, the error of the accumulated solar irradiance, and the error of the area of the photovoltaic array, respectively. From the system cooling capacity expression given by equation (6), it can be known that the test of system performance involves the measurement of temperature and mass, and the measurement of $w_{Q_{ref}}$ can also be analogous to the calculation of equation (10).

$$w_{Q_{ref}} = \sqrt{\sum\left(\frac{\partial w_{Q_{ref}}}{\partial m_i} w_{m_i}\right)^2 + \sum\left(\frac{\partial w_{Q_{ref}}}{\partial T_i} w_{T_i}\right)^2}. \tag{11}$$

In formula (11), w_{m_i} and w_{T_i} represent the measurement error of mass and temperature, respectively. The measurement uncertainty of parameters such as solar radiation, ambient temperature, the mass of ice, photovoltaic modules output current, and voltage in the experiment are determined by the measurement accuracy of the instrument. The parameters are shown in Tables 1 and 2. Substituting the values, the $w_{Q_{ref}}$ is calculated to be about 0.51%; and then substituting into formula (10), the error w_{COP} of the system COP is about 1.22%. It shows that the experimental platform test in this study has high measurement accuracy and the experimental results are reliable.

3. Experimental Results and Analysis

3.1. Photoelectric Performance Analysis of the System under Different PV Capacities. Three sets of PV capacity of 4.5 kW, 5.4 kW, and 6.6 kW were used as driving power sources to drive the vapour-compressed refrigeration subsystem with a 4.4 kW compressor-rated power. The refrigeration performance of the PV refrigerated warehouse system under the three sets of different PV capacities was studied in direct-drive mode. The changes in solar radiation intensity,

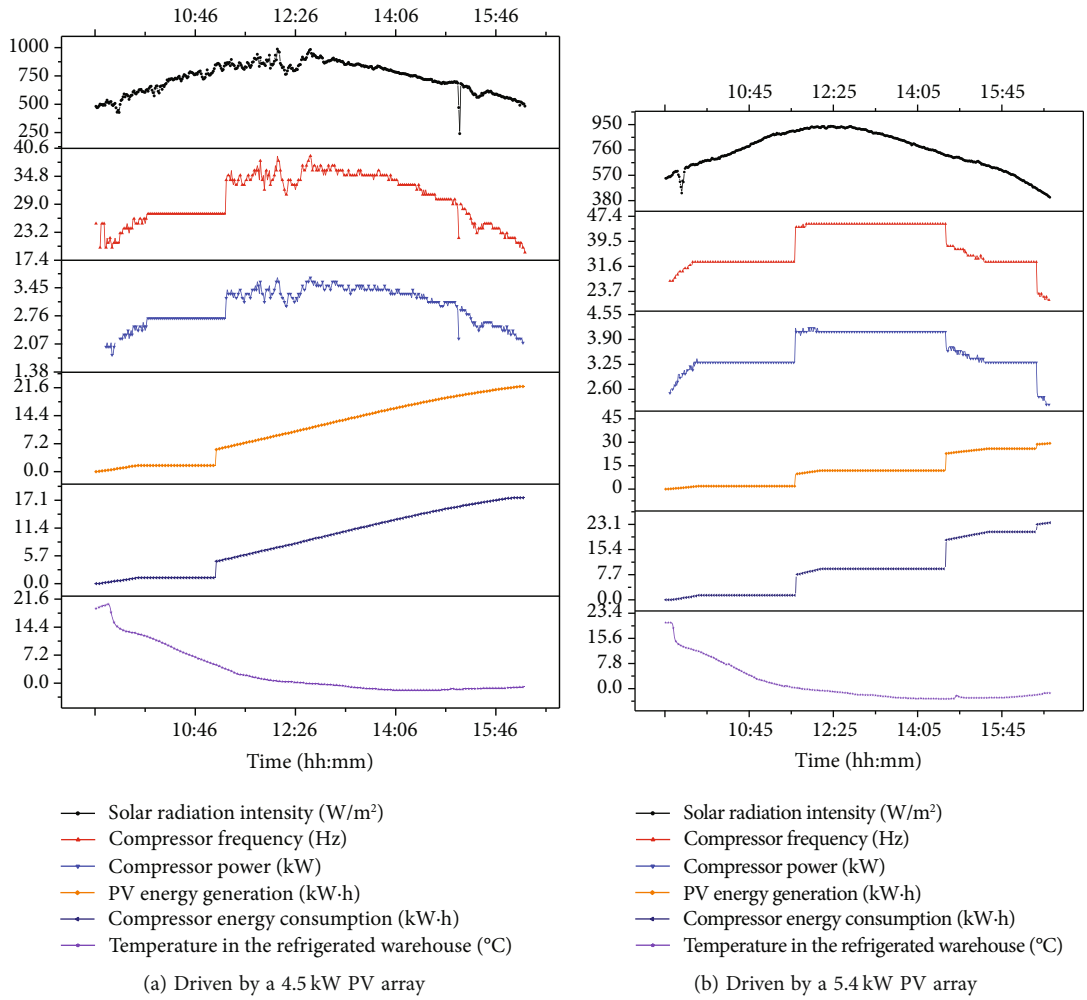

(a) Driven by a 4.5 kW PV array

(b) Driven by a 5.4 kW PV array

Figure 2: Continued.

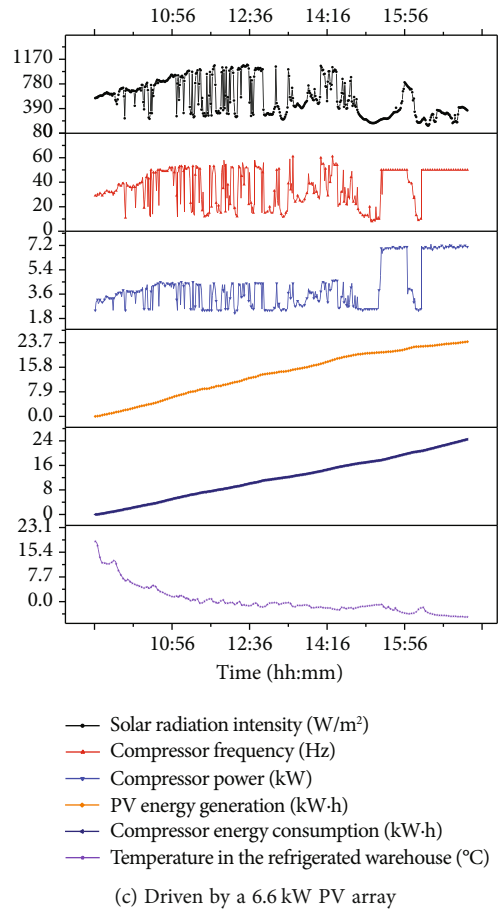

(c) Driven by a 6.6 kW PV array

Figure 2: Changes in system operation performance parameters with different PV capacities.

Table 3: The photoelectric performance characteristic of the system is driven by different PV capacities.

PV power/kW	η_{PV}/%	η/%	ε_I/%	ε_U/%
4.5	17.19	80.7	9.78	0.26
5.4	17.35	81.0	7.56	0.54
6.6	15.38	81.4	5.50	0.48

compressor frequency, compressor power, PV energy generation, compressor energy consumption, and temperature in the refrigerated warehouse during the experiment with different PV capacities are shown in Figure 2.

As can be seen in Figure 2(a), when the solar irradiance reaches 481 W/m^2, the compressor frequency reaches 20 Hz and the compressor starts to operate, at this time, the power is approximately 2.0 kW. The maximum irradiance of the system during operation is 987 W/m^2 throughout the day, the frequency of the compressor is 39 Hz, and the power of the compressor is 3.7 kW. It can be seen in Figure 2(b) that with a 5.4 kW PV capacity when solar irradiance reaches 547 W/m^2, the compressor starts to operate at a frequency of 20 Hz and a power of 2.0 kW. During the experiment, the maximum real-time power of the compressor appears at 12:06, and the maximum value is 4.2 kW. At this time, the compressor frequency is 45 Hz and the instantaneous

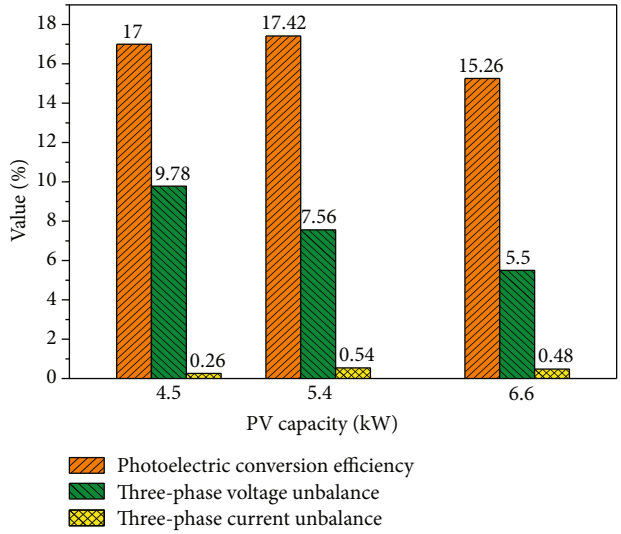

Figure 3: The electronic performance of the system is driven by different PV capacities.

solar irradiance is 934 W/m^2. Figure 2(c) shows that the PV capacity of the system is 6.6 kW. When the solar irradiance reaches 555 W/m^2, the frequency is 29 Hz and the power of the compressor is 2.4 kW. The highest instantaneous irradiance during operation is 1082 W/m^2, the

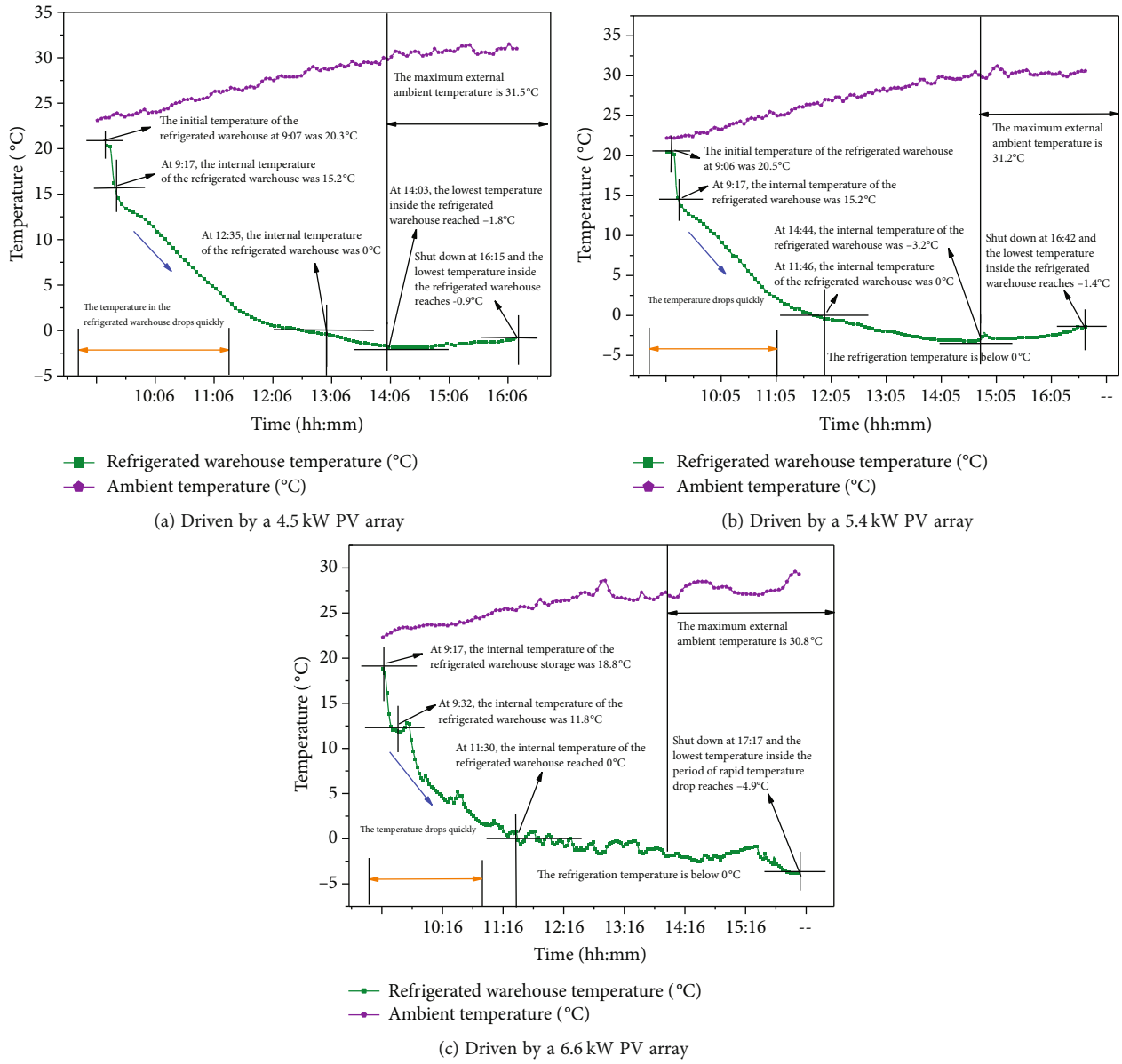

(a) Driven by a 4.5 kW PV array

(b) Driven by a 5.4 kW PV array

(c) Driven by a 6.6 kW PV array

Figure 4: Variation of ambient temperature and storage temperature under different PV power.

compressor frequency is 52 Hz, and the power of the compressor is 4.4 kW. During the experiment, the maximum compressor frequency at 12:27 is 58 Hz, the compressor power is 4.4 kW, and the instantaneous irradiance is 1054 W/m^2.

In the PV direct-drive mode, the PV refrigerated warehouse system enables the compressor to achieve driving automatic operation in the instantaneous irradiance range of 435-555 W/m^2 with a PV capacity of 4.5-6.6 kW. The results of the experiment show that for every 10% increase in α, the solar radiation required to maintain the compressor at the same frequency is reduced by 7.8%.

Table 3 shows the photoelectric performance characteristics of the system driven by different PV capacities. It can be seen from Table 3 that the whole-day utilization efficiency of the compressor is between 80.7% and 81.4% under three different PV capacities; the unbalance of the three-phase current is between 5.50% and 9.78%, and the unbalance of the three-phase voltage is between 0.26% and 0.54%. The photoelectric conversion efficiency is between 15.38% and 17.35%. Figure 3 shows the changes in electrical performance parameters when driven by different PV capacities. As can be seen in Figure 3, when the system is driven by 5.4 kW, the highest photoelectric performance is 17.35%.

3.2. Performance of the Refrigeration of the System under Different PV Capacities. Figure 4 shows the changes in ambient temperature and the refrigeration temperature in the refrigerated warehouse with time when the system is driven by different PV capacities. As can be seen in Figure 4, when three different PV capacities are used as driving power sources, the internal refrigeration temperature of the

Table 4: Experimental results driven by different PV capacities.

PV power/kW	Total radiation/MJ	Run time/h	Time to reach 0°C/min	Stored cold energy available duration/h	Total energy generation/kW·h	Total energy consumption/kW·h	Ice mass/kg	Q_{ave}/kJ/(m^3. Min)	Refrigerating capacity/MJ	The proportion of cold storage energy/%	EER	COP
4.5	463.64	7.1	207	9.8	21.9	17.6	80.4	7.97	83.1	32.41	1.31	0.18
5.4	577.64	7.6	150	17.3	29.3	23.5	144.1	10.11	112.8	42.80	1.33	0.19
6.6	568.09	8.0	133	13.5	22.9	18.6	125.1	8.47	99.5	42.12	1.50	0.19

refrigerated warehouse system can reach below 5°C, which meets the refrigeration temperature requirements of fruits and vegetables. When the system is driven by a 4.5 kW PV array, the temperature in the refrigerated warehouse reaches 0°C after 3.5 h of the startup, and the lowest temperature reaches -3.2°C. The average cooling capacity per unit volume is 7.97 kJ/(m^3·min). In the initial stage of system startup, the cooling rate is the fastest, reaching 0.51°C/min. When the system is driven by a 4.5 kW PV array, the temperature reaches 0°C after 2.67 h of the startup, and the lowest internal temperature is -1.4°C. The average cooling capacity per unit volume reaches 10.11 kJ/(m^3·min). When 6.6 kW of PV power is connected, the temperature reaches 0°C after 2.25 h of startup and the lowest internal refrigeration temperature reaches -4.9°C. The average cooling capacity per unit volume is 8.47 kJ/(m^3·min). The temperature change trend of the refrigerated warehouse reflects the refrigeration performance of the system. From the above experimental analysis, it is concluded that for every 10% increase of α, the time required for the temperature of the refrigerated warehouse to drop to 0°C decreases by 32 min on average.

Figures 4(a)–4(c) show that the internal refrigeration temperature of the refrigerated warehouse has been declining, and the cooling rate is fast at first, and then cooling rate is slow. This is because when the air cooler starts to run, the temperature difference between the air outlet temperature of the air cooler and the internal temperature of the refrigerated warehouse is large, the heat transfer rate is fast, and the sensible heat inside the refrigerated warehouse is quickly taken away. As the internal temperature of the refrigerated warehouse gradually decreases and then becomes closer to the temperature of the air cooler, the temperature difference is smaller and the sensible heat inside the refrigerated warehouse becomes smaller. Additionally, the ambient temperature is higher in the afternoon, and the heat transfer capacity of the condenser from the air is weakened, resulting in a lower cooling rate.

Table 4 shows the experimental results driven by different PV capacities. It can be seen from the table that the mass of ice produced by the system is 80.4-144.1 kg, the COP of the system is between 0.18 and 0.19, and the mass of ice produced increases with the photovoltaic capacity in the PV direct-drive mode. The EER of the refrigeration cycle is 1.31-1.50. With 5.4 kW PV capacity, the maximum average cooling capacity per unit space and time is 10.11 kJ/(m^3·min).

Combined with the analysis of the PV performance characteristics of the system under different PV capacities in Table 3, the photoelectric conversion efficiency of the PV modules can reach 17.35%. It can be seen that 5.4 kW is the more suitable PV power supply capacity for the PV refrigerated warehouse system among the three different PV capacities. From the analysis of the system operating data, it can be found that the energy utilization efficiency of the PV direct-drive refrigerated warehouse system is affected by multiple factors such as photoelectric efficiency, EER, and meteorological conditions. As the ratio of PV capacity to compressor-rated power α gradually increases from 1, the system EER and COP increase gradually, and the growth rate of COP is extremely slow when α reaches 1.3.

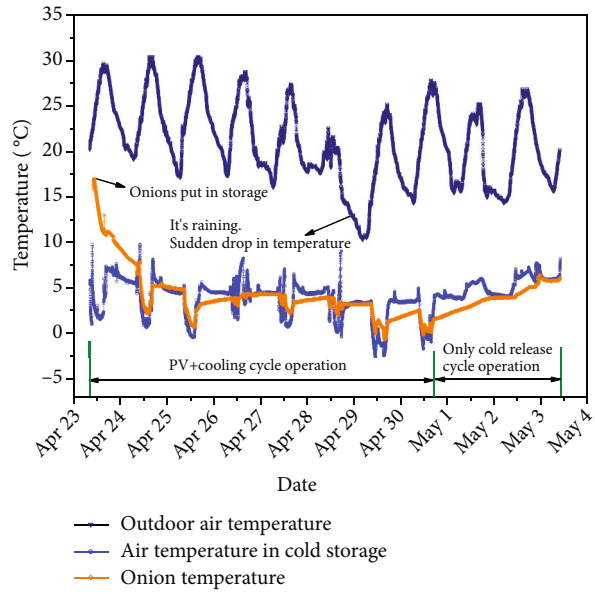

Figure 5: Variation of air temperature in the refrigerated warehouse, load temperature, and the ambient temperature outside cold storage.

The system operates under different PV capacities showing that increasing the capacity of PV modules in the system can reduce the time required to reach 0°C in cold storage. When the system works near the optimal ratio of PV capacity to compressor-rated power, the time to get 0°C in the refrigerated warehouse can be shortened by about 35 min for each additional 1 kW photovoltaic module. The proportion of stored cold energy to total cooling capacity and the duration of available cold energy increases with the system capacity ratio, but there is no significant change after reaching the optimal ratio of PV capacity to compressor power. Considering that the growth rate of the system COP also slows down, the PV module capacity exceeding the optimal ratio of PV capacity to compressor-rated power of the system has no positive effect on the system refrigeration performance.

3.3. Continuous Operation Experiment with Load Driven by 5.4 kW. To further obtain the operating performance of the system with load, the refrigerated warehouse system experiment was carried out with 500 kg onions as load. After placing the onions in a natural ventilated environment outside the refrigerated warehouse for two days, the onions with a total weight of 500 kg were placed in the basket at approximately 10:00 am on 23 April 2021 and placed in the cold storage, the refrigerated warehouse continued to operate until May 3.

Temperature and humidity sensors were placed at different positions in the refrigerated warehouse and at different positions of the loaded onions to monitor the temperature and humidity during the experiment. The experimental results showed that there were few differences in temperature and humidity in different positions of the onion, which was approximately 0.2°C. The changes in air temperature in the

Table 5: Initial investment cost of the photovoltaic direct-drive refrigerated warehouse system (unit: thousand yuan).

PV subsystem			Enclosure and refrigeration unit			Auxiliary materials			Transportation and installation	Total
PV modules	Controllers	Inverters	Enclosure structure	Refrigeration units	Instrumentation	Bracket	Cables and pipes	Control cabinet	Transportation and installation	46.5
21.6	1.5	1.7	7.5	5.5	0.7	2.0	2.0	1.0	3.0	

refrigerated warehouse, the average onion temperature in each position, and the outside ambient temperature of the refrigerated warehouse during the experiment are shown in Figure 5.

As can be seen in Figure 5, the temperature of the onions before storage is 17°C, which is 14°C higher than the air temperature in the refrigerated warehouse. Then the temperature of the onions gradually decreased to almost the same temperature as the air in the refrigerated warehouse. After that, the onion temperature and the air temperature in the refrigerated warehouse showed the same trend of change, but the onion temperature changed less. That is because the specific heat capacity of the air is much smaller than that of the load. After the system has been running continuously for eight days, after the refrigeration cycle was closed, the temperature-changing trend of air in the refrigerated warehouse was quite different from that of the onion. The air temperature in the refrigerated warehouse had the same trend of change as the temperature at night and day, while the onion temperature rose slowly. After closing the refrigeration cycle at 17:05 on 30 April, only the cooling release cycle was operated and it reached 6.2°C at 10:20 am on May 3, then ending the experiment.

4. System Economic Analysis

The investment cost of the solar photovoltaic direct-drive refrigerated warehouse system with ice thermal energy storage C_{total} is mainly composed of three parts: the initial investment cost of the system C_s, the operation and maintenance cost during the service life C_{om}, and the nonrecurring cost during the service life C_{ac}.

Among them, the initial investment cost of the solar photovoltaic direct-drive refrigerated warehouse system with ice thermal energy storage C_s mainly includes the costs of equipment, accessories, transportation and installation, and auxiliary materials. The operation and maintenance cost C_{om} mainly consist of cold energy storage medium or batteries that need to be replaced regularly during the service life of the system, as well as the consumables in the process of use, etc. The nonrecurring costs C_{ac} are mainly the maintenance or replacement of unpredictable and probabilistic equipment failure parts, generally 15% to 25% of the initial equipment cost. The present value of the total investment cost of the solar photovoltaic direct-drive refrigerated warehouse system with ice thermal energy storage can be obtained by converting and adding to the operation and maintenance cost and nonrecurring cost of the system during the service period into the initial investment cost.

The volume of the solar photovoltaic direct-drive refrigerated warehouse constructed in this paper is 30 m^3. The difference between the annual average temperature and the cold storage temperature in Kunming, China, where the cold storage is located and calculated as 15°C, the daily average peak sunshine is 4.5 hours, and the system guarantee coefficient is 1.2. The energy efficiency ratio of the compression refrigeration subsystem is estimated at 2.5, the system is equipped with a 5.4 kW independent photovoltaic array. Based on the PV module price of 4 yuan/W when the system was built, the cost of PV modules was 21,600 yuan. The initial investment required for the system is shown in Table 5.

The economic benefits of the system come from the revenue from refrigerated items. According to the current cold storage charge of 4-4.5 yuan/(ton·day) in Kunming and estimated according to the comprehensive utilization rate of 50% of the refrigerated warehouse volume, the photovoltaic direct-drive refrigerated warehouse system constructed in this paper can recover the initial investment cost in 6-6.5 years.

The service life of photovoltaic modules is about 25 years, and the service life of other equipment in the photovoltaic direct-drive refrigerated warehouse system is generally shorter than that of photovoltaic modules. According to the comprehensive use of the system for 20 years, the net income of the average cold storage per cubic meter volume is about 3.2-3.3 thousand yuan/m^3, which is 2.2 times the investment of the refrigerated warehouse per unit volume.

5. Conclusions

In this paper, a PV refrigerated warehouse system with ice thermal energy storage is constructed, and the performance of the system under different PV capacities is studied. The photoelectric performance and refrigeration performance of the system are analysed. The conclusions are as follows:

(1) In the PV direct-drive mode of 4.5-6.6 kW, the instantaneous irradiance for the compressor to achieve automatic drive operation is 435-555 W/m^2, and the internal temperature of the refrigerated warehouse meets the requirements of fruit and vegetable refrigeration. With 5.4 kW of PV capacity, the average cooling capacity per unit of space and time of the refrigerated warehouse system is the highest, which is 10.11 kJ/(m^3·min)

(2) The whole-day utilization efficiency of the compressor is between 80.7% and 81.4% under different PV capacities, the unbalance of the three-phase current is between 5.50% and 9.78%, and the unbalance of

the three-phase voltage is between 0.26% and 0.54%. The photoelectric conversion efficiency is 15.38%-17.35%

(3) When the ratio of PV capacity to compressor-rated power of the system increases by 10%, the intensity of solar radiation required for the compressor to work at the same frequency decreases by about 7.8%; the average time required for the temperature of the refrigerated warehouse to drop to 0°C is reduced by 32 min. The EER of the vapour-compressed refrigeration system and the COP of the refrigerated warehouse system increase with the ratio of PV capacity to compressor-rated power α from 1. When α increases to 1.3, the COP growth rate is very slow. For the PV direct-drive ice thermal energy storage refrigerated warehouse system with a compressor-rated power of 4.4 kW, the suitable ratio of PV capacity to compressor-rated power α is about 1.3

(4) The refrigerated warehouse system is driven by 5.4 kW and can run continuously and stably with load under different weather conditions. Under the mode of refrigeration and cold energy storage during the day and only the cold release cycle at night, the stored cold energy can still meet the refrigeration required by the load for 48 hours after eight days of continuous operation. According to the current market price of cold storage, during the service life of the system, the income per unit volume of cold storage is about 2.2 times the investment

Data Availability

Data references are described in the text of the article.

Conflicts of Interest

The authors declare that they have no conflict of interest.

Acknowledgments

This research was funded by the Yunnan Power Grid Corporation Science and Technology Project (grant number YNKJXM20190087).

References

[1] D. K. Liu, C. C. Xu, C. X. Guo, and X. X. Zhang, "Sub-zero temperature preservation of fruits and vegetables: a review," *Journal of Food Engineering*, vol. 275, p. 109881, 2020.

[2] R. D. Raut, B. B. Gardas, V. S. Narwane, and B. E. Narkhede, "Improvement in the food losses in fruits and vegetable supply chain - a perspective of cold third-party logistics approach," *Operations Research Perspectives*, vol. 6, article 100117, 2019.

[3] S. F. Santosdos, R. Cardoso, Í. M. P. Borges et al., "Post-harvest losses of fruits and vegetables in supply centers in Salvador, Brazil: analysis of determinants, volumes and reduction strategies," *Waste Management*, vol. 101, pp. 161–170, 2020.

[4] S. Tim, C. Hanson, J. Ranganathan et al., *Creating a sustainable food future; World Resources Institute*, World Resources Institute, Washington DC, 2019.

[5] H. Zhao, S. Liu, C. Tian, G. Yan, and D. Wang, "Tour d'horizon de l'etat actuel de la chaine du froid en Chine," *International Journal of Refrigeration*, vol. 88, pp. 483–495, 2018.

[6] N. Aste, C. Del Pero, and F. Leonforte, "Active refrigeration technologies for food preservation in humanitarian context - a review," *Sustainable Energy Technologies and Assessments*, vol. 22, pp. 150–160, 2017.

[7] "Application of new physical storage technology in fruit and vegetable industry," *Journal of Biotechnology*, vol. 11, no. 25, pp. 6718–6722, 2012.

[8] R. M. Lazzarin and M. Noro, "Past, present, future of solar cooling: technical and economical considerations," *Solar Energy*, vol. 172, pp. 2–13, 2018.

[9] Y. Xu, X. Ma, R. H. E. Hassanien, X. Luo, G. Li, and M. Li, "Performance analysis of static ice refrigeration air conditioning system driven by household distributed photovoltaic energy system," *Solar Energy*, vol. 158, pp. 147–160, 2017.

[10] Y. Li and R. Z. Wang, "Photovoltaic-powered solar cooling systems," in *Advances in Solar Heating and Cooling*, pp. 227–250, Woodhead Publishing, 2016.

[11] A. Modi, A. Chaudhuri, B. Vijay, and J. Mathur, "Performance analysis of a solar photovoltaic operated domestic refrigerator," *Applied Energy*, vol. 86, no. 12, pp. 2583–2591, 2009.

[12] B. J. Huang, T. F. Hou, P. C. Hsu et al., "Design of direct solar PV driven air conditioner," *Renewable Energy*, vol. 88, pp. 95–101, 2016.

[13] Y. Han, M. Li, Y. Wang et al., "Impedance matching control strategy for a solar cooling system directly driven by distributed photovoltaics," *Energy*, vol. 168, pp. 953–965, 2019.

[14] P. J. Axaopoulos and M. P. Theodoridis, "Design and experimental performance of a PV ice-maker without battery," *Solar Energy*, vol. 83, no. 8, pp. 1360–1369, 2009.

[15] V. Torres-Toledo, K. Meissner, P. Täschner, S. Martınez-Ballester, and J. Müller, "Design and performance of a small-scale solar ice-maker based on a DC-freezer and an adaptive control unit," *Solar Energy*, vol. 139, pp. 433–443, 2016.

[16] S. Kaplanis and N. Papanastasiou, "The study and performance of a modified conventional refrigerator to serve as a PV powered one," *Renewable Energy*, vol. 31, no. 6, pp. 771–780, 2006.

[17] H. Lei, W. Guo, and C. Dai, "Experimental study of a micro-refrigeration system driven by photovoltaic power generation," *Energy Procedia*, vol. 158, pp. 516–521, 2019.

[18] V. Torres-Toledo, K. Meissner, A. Coronas, and J. Müller, "Caracterisation de la performance d'un petit systeme de refroidissement de lait avec stockage de glace pour les applications photovoltaiques," *International Journal of Refrigeration*, vol. 60, pp. 81–91, 2015.

[19] V. Torres-Toledo, A. Hack, F. Mrabet, A. Salvatierra-Rojas, and J. Müller, "Solution de refroidissement du lait a la ferme grace a des bidons isothermes avec compartiment a glace integre," *International Journal of Refrigeration*, vol. 90, pp. 22–31, 2018.

[20] E. M. Salilih and Y. T. Birhane, "Modelling and performance analysis of directly coupled vapor compression solar refrigeration system," *Solar Energy*, vol. 190, pp. 228–238, 2019.

[21] A. A. M. El-Bahloul, A. H. H. Ali, and S. Ookawara, "Performance and sizing of solar driven dc motor vapor compression

refrigerator with thermal storage in hot arid remote areas," *Energy Procedia*, vol. 70, pp. 634–643, 2015.

[22] R. Mishra, S. K. Chaulya, G. M. Prasad, S. K. Mandal, and G. Banerjee, "Design of a low cost, smart and stand-alone PV cold storage system using a domestic split air conditioner," *Journal of Stored Products Research*, vol. 89, article 101720, 2020.

[23] M. Hoseini Rahdar, A. Emamzadeh, and A. Ataei, "A comparative study on PCM and ice thermal energy storage tank for air- conditioning systems in office buildings," *Applied Thermal Engineering*, vol. 96, pp. 391–399, 2016.

[24] X. Wang and M. Dennis, "A comparison of battery and phase change coolth storage in a PV cooling system under different climates," *Sustainable Cities and Society*, vol. 36, pp. 92–98, 2018.

[25] C. Luerssen, O. Gandhi, T. Reindl, C. Sekhar, and D. Cheong, "Levelised cost of storage (LCOS) for solar-PV-powered cooling in the tropics," *Applied Energy*, vol. 242, pp. 640–654, 2019.

[26] S. A. Ghoreishi-Madiseh, A. F. Kuyuk, H. Kalantari, and A. P. Sasmito, "Ice versus battery storage; a case for integration of renewable energy in refrigeration systems of remote sites," *Energy Procedia*, vol. 159, pp. 60–65, 2019.

[27] Y. Xu, M. Li, X. Luo et al., "Étude experimentale sur un systeme de conditionnement d'air photovoltaique solaire a stockage thermique de glace," *International Journal of Refrigeration*, vol. 86, pp. 258–272, 2018.

[28] Y. Xu, M. Li, and R. H. E. Hassanien, "Energy conversion and transmission characteristics analysis of ice storage air conditioning system driven by distributed photovoltaic energy system," *International Journal of Photoenergy*, vol. 2016, Article ID 4749278, 17 pages, 2016.

[29] S. Components, "Symmetrical components: as applied to the analysis of unbalanced electrical circuits," *Nature*, vol. 132, no. 3345, pp. 876–876, 1933.

[30] A. Khanlari, H. Ö. Güler, A. D. Tuncer et al., "Experimental and numerical study of the effect of integrating plus-shaped perforated baffles to solar air collector in drying application," *Renewable Energy*, vol. 145, pp. 1677–1692, 2020.

[31] M. Yahya, H. Fahmi, A. Fudholi, and K. Sopian, "Performance and economic analyses on solar-assisted heat pump fluidised bed dryer integrated with biomass furnace for rice drying," *Solar Energy*, vol. 174, pp. 1058–1067, 2018.